International Journal of Solids and Structures 50 (2013) 4270–4278

Contents lists available at ScienceDirect

International Journal of Solids and Structures

journal homepage: www.elsevier.com/locate/ijsolstr

Dynamic fracture of concrete compact tension specimen: Experimental and numerical study

Joško Ožbolt *, Josipa Bošnjak, Emiliano Sola

Institute of Construction Materials, University of Stuttgart, 70560 Stuttgart, Germany

ARTICLE INFO

Article history:
Received 11 June 2013
Received in revised form 9 August 2013
Available online 3 September 2013

Keywords:
Concrete
Compact tension specimen
Dynamic fracture
Experiments
Finite element analysis
Rate sensitivity
Structural inertia
Crack branching

ABSTRACT

Compared to quasi-static loading concrete loaded by higher loading rates acts in a different way. There is an influence of strain-rate and inertia on resistance, failure mode and crack pattern. With increase of loading rate failure mode changes from mode-I to mixed mode. Moreover, theoretical and numerical investigations indicate that after the crack reaches critical velocity there is progressive increase of resistance and crack branching. These phenomena have recently been demonstrated and discussed by Ožbolt et al. (2011) on numerical study of compact tension specimen (CTS) loaded by different loading rates. The aim of the present paper is to experimentally verify the results obtained numerically. Therefore, the tests and additional numerical studies on CTS are carried out. The experiments fully confirm the results of numerical prediction discussed in Ožbolt et al. (2011). The same as in the numerical study it is shown that for strain rates lower than approximately 50/s the structural response is controlled by the rate dependent constitutive law, however, for higher strain rates crack branching and progressive increase of resistance is observed. This is attributed to structural inertia and not the rate dependent strength of concrete. Maximum crack velocity of approximately 800 m/s is measured before initiation of crack branching. The comparison between numerical and experimental results shows that relatively simple modeling approach based on continuum mechanics, rate dependent microplane model and standard finite elements is capable to realistically predict complex phenomena related to dynamic fracture of concrete.

1. Introduction

From experimental, theoretical and numerical studies of concrete structures is well known that the resistance, failure mode, crack pattern and crack velocity are influenced by loading rate (Freund, 1972a,b; Dilger et al., 1978; Banthia et al., 1987;Reinhardt, 1982; Bischoff and Perry, 1991; Weerheijm, 1992; Ožbolt and Reinhardt, 2005; Ožbolt et al., 2006; Larcher, 2009; Pedersen, 2009; *fib*, 2012; Ožbolt et al., 2011; Ožbolt and Sharma, 2012). It can be stated that the rate dependent response of concrete is controlled through three different effects: (i) through the rate dependency of the growing microcracks (influence of inertia at the micro-crack level), (ii) through the viscous behavior of the bulk material between the cracks (viscosity due to the water content) and (iii) through the influence of structural inertia forces. From the numerical point of view, assuming macro or meso scale analysis, the first two effects can be accounted for by the constitutive law and the third effect should be automatically accounted for through dynamic analysis where the constitutive law interacts with structural inertia forces (Ožbolt et al., 2011). Depending on the material type and the loading rate, the first, second or third effect may dominate. For quasi-brittle materials, such as concrete, which exhibit cracking and damage phenomena, the first two effects are important for relatively low and medium loading rates. However, in case of higher loading rates (impact) the last effect seems to be dominant, although the other effects cannot be neglected.

Principally, with increase of loading rate failure mode tends to change from mode-I to mixed mode. As discussed by Ožbolt et al. (2011) and Ožbolt and Sharma (2012), responsible for this is structural inertia, which homogenize the material in the impact zone and force damage (crack) to move away from the zone of high inertia forces. Furthermore, when crack starts to propagate relatively fast, inertia forces at the crack tip tends to prevent crack propagation. Consequently, single crack split into two inclined cracks. This phenomenon is known as crack branching. The crack velocity also depends on loading rate. The maximal theoretical crack velocity is Rayleigh wave speed $v_R = C_R(G_c/\rho_c)^{0.5}$ where the constant C_R depends on Poisson's ratio, G_c is the shear modulus and ρ_c is specific weight of the material. For normal strength

* Corresponding author. Tel.: +49 71168563330; fax: +49 71168563349.
E-mail addresses: ozbolt@iwb.uni-stuttgart.de (J. Ožbolt), josipa.bosnjak@iwb.uni-stuttgart.de (J. Bošnjak), emiliano.sola@iwb.uni-stuttgart.de (E. Sola).

0020-7683/$ - see front matter © 2013 Elsevier Ltd. All rights reserved.
http://dx.doi.org/10.1016/j.ijsolstr.2013.08.030

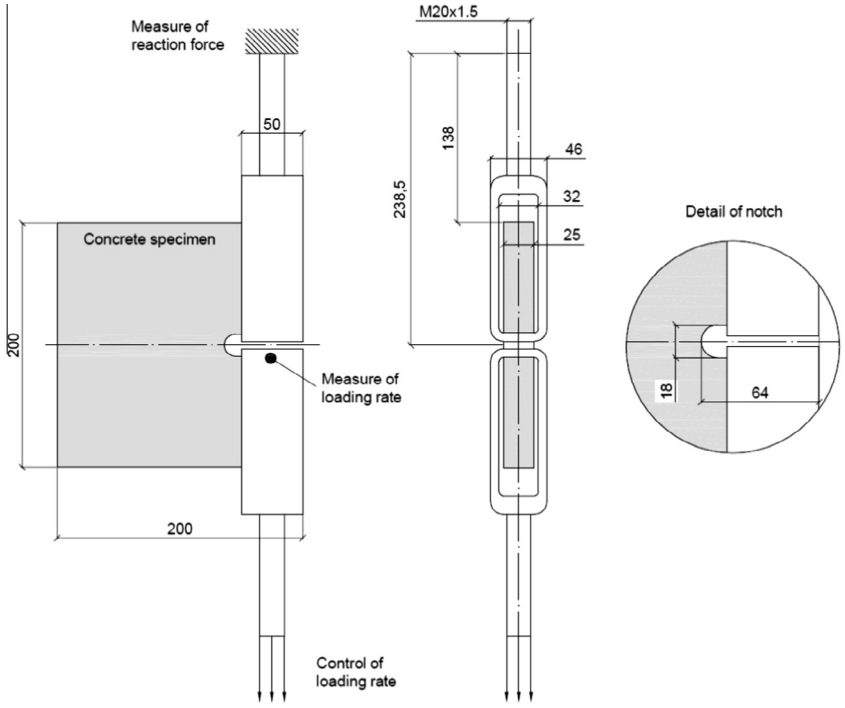

Fig. 1. Geometry of the CTS, top and bottom steel loading frames and detail of notch (all in mm).

concrete Rayleigh wave speed is approximately equal to 2100 m/s. However, experimental (Curbach and Eibl, 1990), theoretical (Freund, 1972a,b) and numerical investigations (Rabczuk and Belytschko, 2004; Rabczuk et al., 2004; Travaš et al., 2009; Ožbolt et al., 2011) indicate that a single mode-I type of crack cannot reach theoretical velocity. According to these investigations the maximal crack speed in normal strength concrete is between 500 and 600 m/s.

Compact tension specimen is in engineering frequently used to determinate fracture properties of concrete, such as tensile strength and fracture energy. In recent theoretical (numerical) study (Ožbolt et al., 2011), the influence of loading rate on the response of CTS of normal strength concrete was investigated. The main conclusions of the study can be summarized as follows. (i) With increase of loading rate the resistance increases approximately linear (in semi-log scale) up to the critical loading rate. In this range of loading rate the rate dependent constitutive law controls the resistance. However, for higher loading rates there is progressive increase of resistance that is controlled mainly by structural inertia. (ii) Crack pattern is rate dependent. For relatively low loading rates there is only one crack that is approximately perpendicular to the loading direction. However, when loading rate reaches approximately 2.5 m/s there is a crack branching and for even higher loading rates multiple crack branching is observed. (iii) For the normal strength concrete (uni-axial compressive strength around 30 MPa) maximum crack velocity of approximately 600 m/s is estimated from the results of the finite element analysis. This velocity is measured before crack branching and once the crack branches the velocity drops down. It was concluded that inertia at the crack tip is responsible for crack branching.

Currently no systematic experimental tests on concrete CTS loaded by different rates exist. This is especially true with respect to the crack velocity and crack branching phenomena. Therefore, to experimentally investigate behavior of CTS under different loading rates and to verify the results of recent theoretical study (Ožbolt et al., 2011) experiments on CTS are carried out. Due to the technical reasons the geometry and loading of the test specimen is not exactly the same as in numerical study. Therefore, the numerical analysis of tested specimen is also carried out using the same finite element code as reported in Ožbolt et al. (2011). In the first part of the paper the test set-up is discussed and the results of experiments are summarized. Subsequently, the experimental results are evaluated, compared with numerical prediction and conclusions are drawn out.

2. Experiment on dynamic fracture of concrete CTS

As mentioned before, to verify numerical results recently published by Ožbolt et al. (2011), experimental tests on concrete CTS are carried out for loading (displacement) rates up to approximately 5 m/s. The experiments are carried out at MPA Institute, University of Stuttgart.

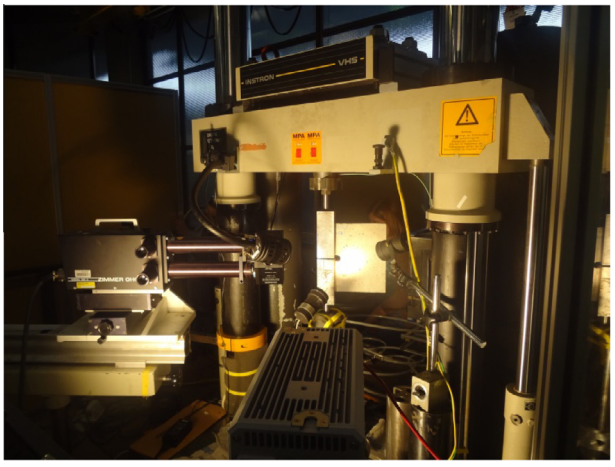

Fig. 2. Test set-up.

Table 1
Summary of experimental results.

Test Nr.	Target displacement rate (m/s)	Measured displacement rate (m/s)	Displacement rate at contact (m/s)	Max. reaction (kN)	Number of cracks
1	0.10	0.079	0.045	2.54	S
2	0.10	0.061	0.035	2.83	S
3	0.50	0.505	0.304	3.47	S
4	1.00	0.815	0.491	4.05	S
5	2.00	1.952	1.375	4.64	S
6	3.00	3.015	1.407	5.76	S
7	3.00	2.863	1.736	4.49	S
8	6.00	5.339	3.268	4.59	B
9	6.00	4.913	3.318	6.88	B
10	8.00	6.732	3.993	4.69	B
11	8.00	6.716	3.967	3.32	MB
12	8.00	6.774	4.298	5.66	B

S = single crack; B = branching; MB = multiple branching.

2.1. Geometry, concrete properties and loading

The dimensions of the tested CTS (Length, Height and Thickness) are: $L \times H \times T = 200 \times 200 \times 25$ mm, the notch length and width are 64 and 18 mm, respectively. The specimen geometry and two steel frames, one loading and another reaction, are shown in Fig. 1. In contrary to the numerical study (Ožbolt et al., 2011), the specimen is tested such that the notch is placed in horizontal position (see Fig. 1). Due to the technical reasons the load is applied only at one (bottom) surface of the notch through displacement control of the bottom loading frame. The top steel frame is fixed at the top and served as reaction. Before the experiment the top and bottom steel frames are glued to the corresponding notch surfaces. The photo of the test set-up is shown in Fig. 2.

The concrete specimens are cured 7 days under constant temperature of 20 °C and relative humidity (RH) of 100%. Subsequently the specimen is approximately three weeks exposed to RH of 60%. The uni-axial compressive strength of concrete is measured before testing on standard cylinders, diameter and height of 150 and 300 mm, respectively. The average strength (three specimens) is $f_c = 53$ MPa. Based on f_c, the concrete properties were estimated as: Young's modulus $E_c = 36$ GPa, Poisson's ratio $\nu = 0.18$, tensile strength $f_t = 3.80$ MPa and fracture energy $G_F = 65$ J/m^2. Mass density of concrete is assumed to be $\rho_c = 2400$ kg/m^3 and maximum

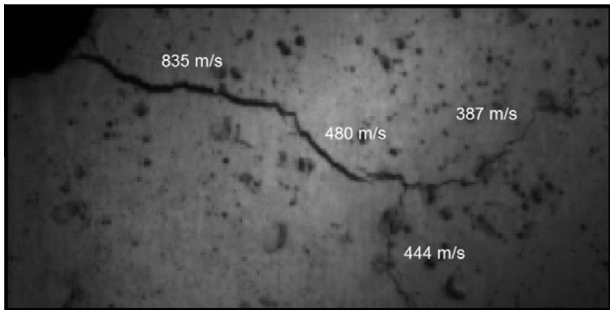

Fig. 4. Crack velocity before and after branching (Test Nr. 12).

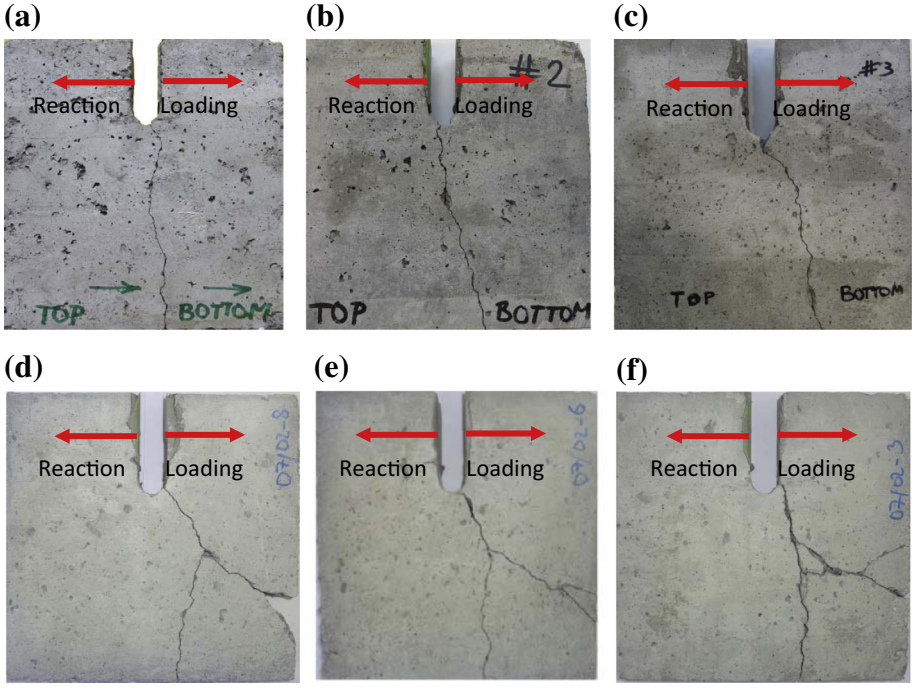

Fig. 3. Experimentally observed crack patterns for displacement rates measured at the contact between bottom loading plate and concrete notch surface: (a) 0.304 m/s, (b) 0.491 m/s, (c) 1.375 m/s, (d) 3.318 m/s, (e) 3.993 m/s and (f) 3.967 m/s.

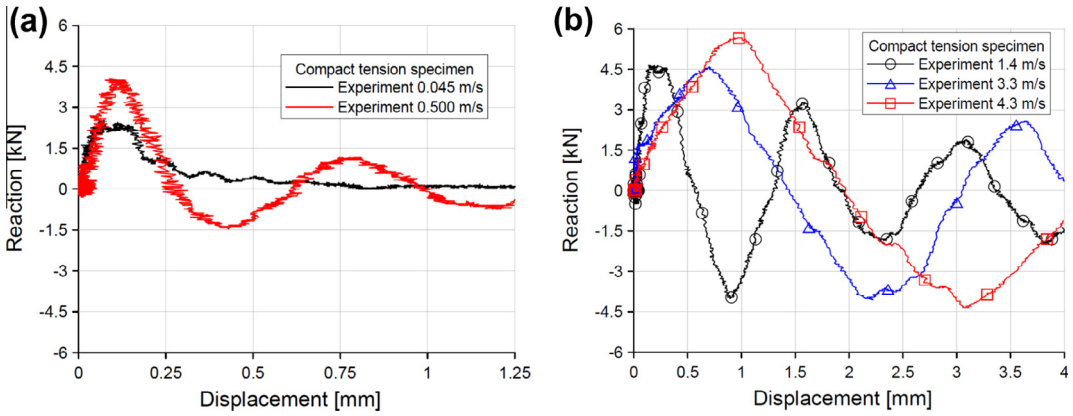

Fig. 5. Experimentally measured reaction-displacement response.

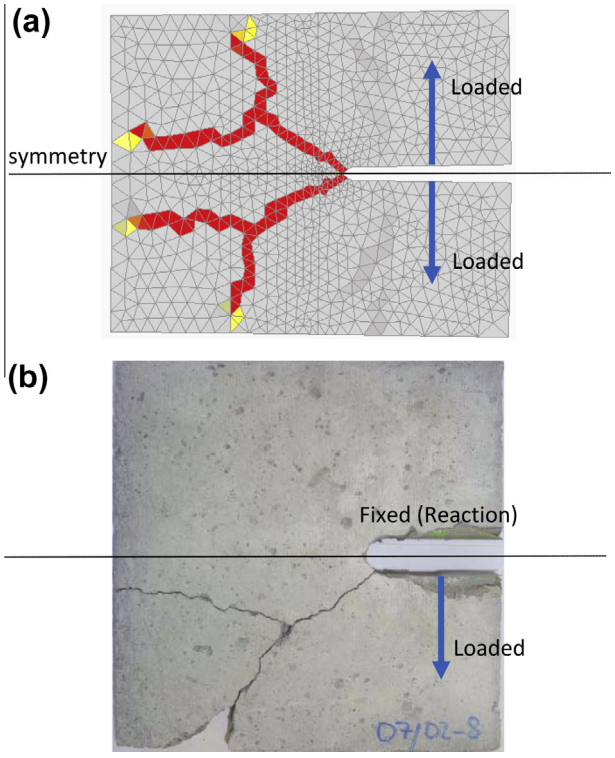

Fig. 6. Crack branching: (a) numerically predicted by Ožbolt et al. (2011) (loading rate 2.50 m/s) and (b) experimentally obtained (loading rate 3.30 m/s).

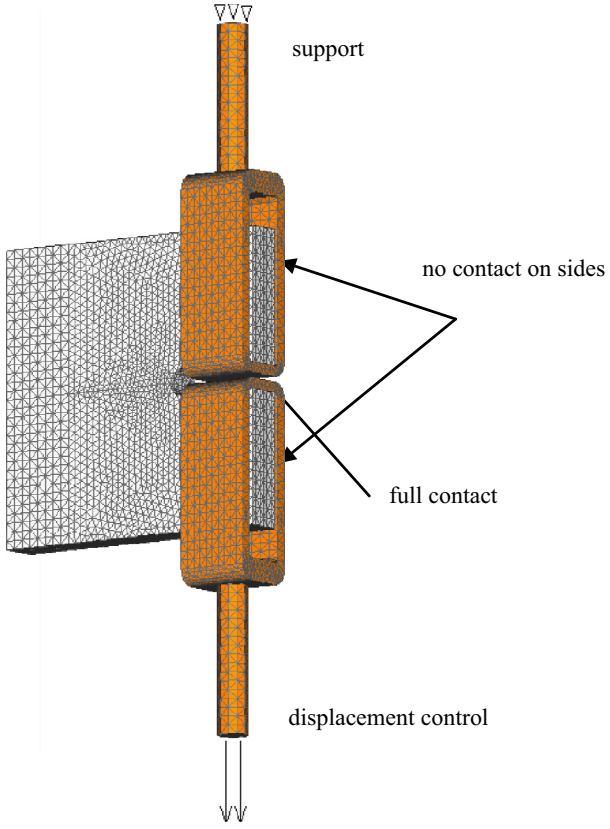

Fig. 7. 3D finite element model of the CTS.

aggregate size is 8 mm. The loading frames were made of normal steel with the following properties: Young's modulus $E_s = 210$ GPa, Poisson's ratio $\nu = 0.33$ and mass density $\rho_s = 7800$ kg/m^3.

In the experiments are measured displacement rate at the application of load (bottom loading frame) and at the contact of the loading frame and concrete. At the top steel frame is monitored the reaction. To estimate the crack velocity, in the zone of cracking the experiment is recorded by high speed camera. Target (projected) loading rates at the point of load application (bottom of the loading frame) are varied from 0.10 m/s up to 8.00 m/s. In total 12 experiments are carried out.

2.2. Evaluation of experimental results

In Table 1 are summarized experimental results obtain from 12 performed tests. Shown are projected (target) displacements

Table 2
Summary of numerical and test results.

Test Nr.	Displacement rate, analysis (m/s)	Displacement rate, test (m/s)	Max. reaction, analysis (kN)	Max. reaction, test (kN)	Number of cracks – test/an
0	Quasi-static	–	1.60	–	–/S
1	0.045	0.045	2.29	2.54	S/S
2	0.035	0.035	2.21	2.83	S/S
3	0.300	0.304	3.65	3.47	S/S
4	0.500	0.491	4.12	4.05	S/S
5	1.400	1.375	3.54	4.64	S/S
8	3.300	3.268	4.76	4.59	B/B
10	4.000	3.993	4.93	4.69	B/B
12	4.300	4.298	5.16	5.66	B/B

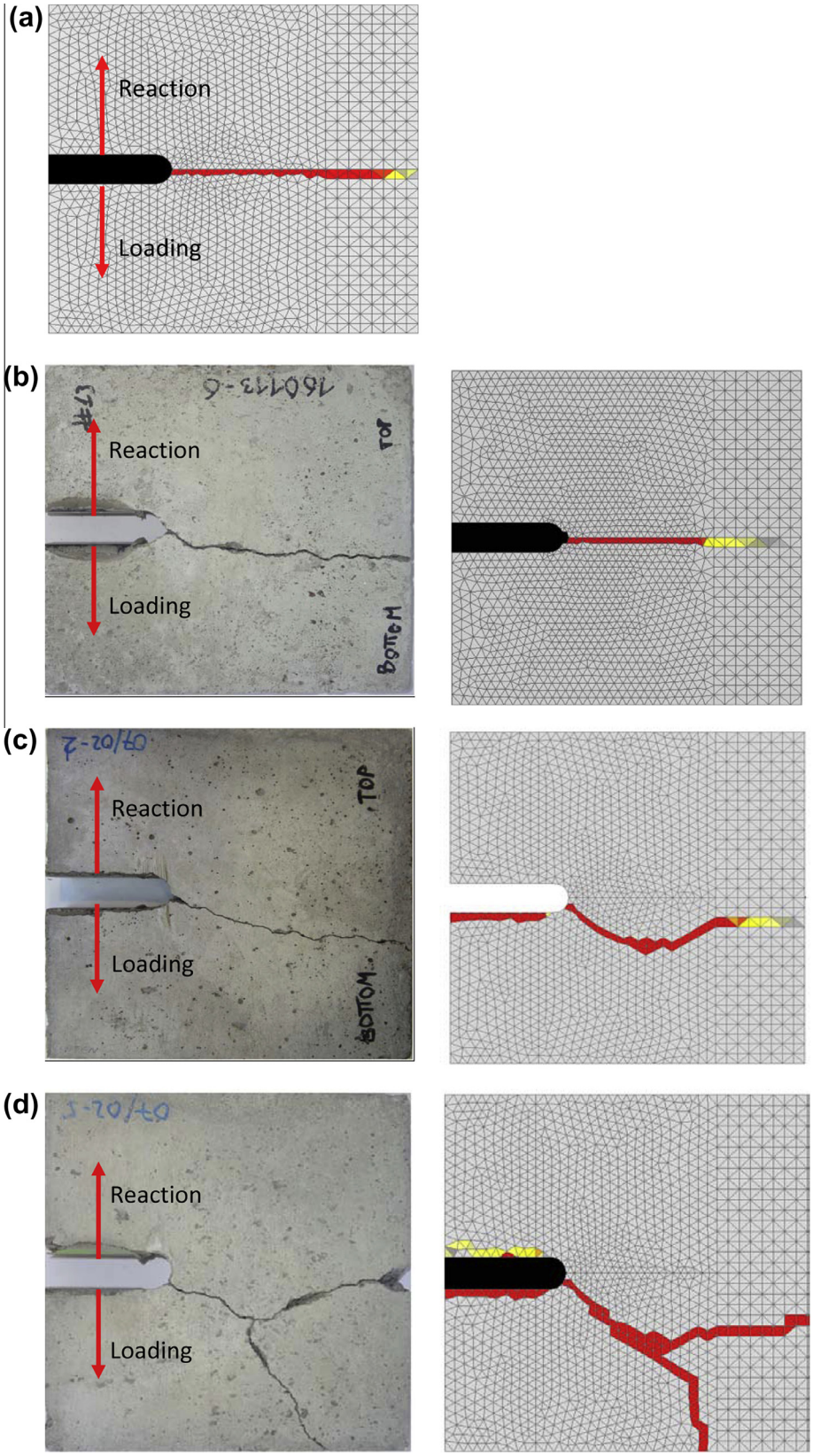

Fig. 8. Experimentally and numerically predicted crack patterns in terms of max. principal strains for: (a) static loading, (b) loading rate 0.035 m/s, (c) 1.40 m/s and (d) 4.30 m/s (red = critical crack opening of 0.20 mm). (For interpretation of the references to colour in this figure legend, the reader is referred to the web version of this article.)

rates applied at the bottom of the loading frame, actual displacement rates at the same place and at the contact between bottom loading frame and concrete, recorded maximum reaction and observed failure mode. Note that the gap in the loading rate between test Nr. 7 and 8 is relatively large, however, the aim of the study was not to exactly detect the loading rate at which

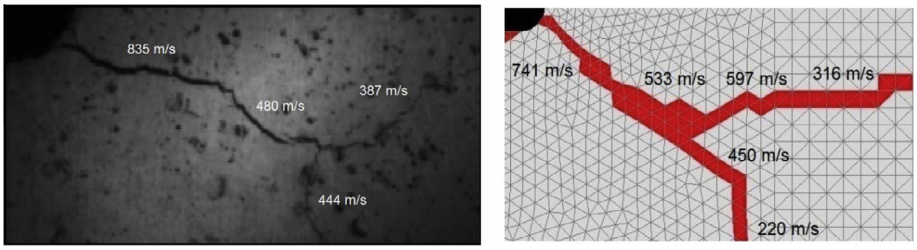

Fig. 9. Measured and numerically predicted crack velocities for loading rate 4.30 m/s.

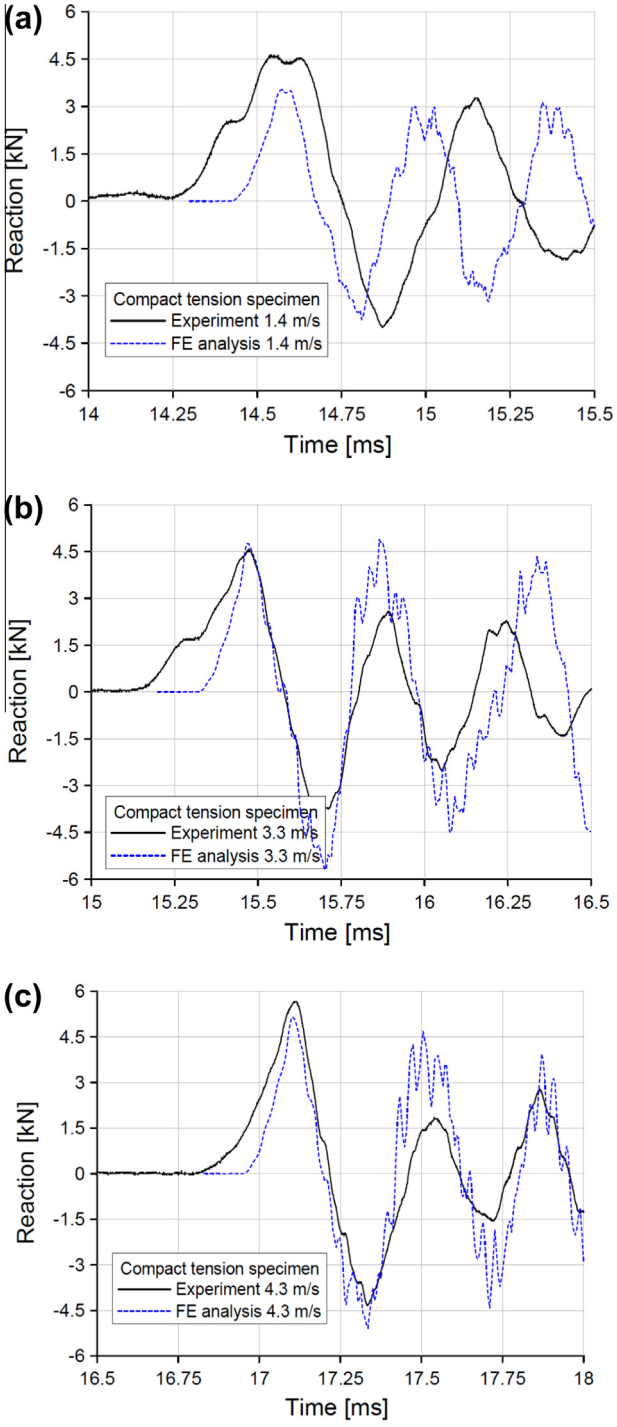

Fig. 10. Measured and numerically predicted reaction-time response for displacement rates: (a) 1.40 *m/s*, (b) 3.30 *m/s*, (c) 4.30 *m/s*.

crack start to branches but to demonstrate experimentally the existence of the phenomena, to confirm the numerical prediction and finally to understand the reason.

In Fig. 3 are shown typical crack patterns for displacement rates measured at the contact between concrete and bottom loading frame. It turns out that for the tested geometry and concrete properties there is only a single crack if the loading is less than approximately 2.0–3.0 m/s. For relative low loading rate, close to quasi-static, the crack propagates almost perpendicular to the loading direction. However, for higher displacement rates the crack becomes inclined with respect to the loading direction. The first crack branching is observed for displacement rate of approximately 3.30 m/s and for higher displacement rates (approximately 4.0 m/s) even multiple crack branching is observed.

The crack velocity is estimated from the evaluation of photos obtain from high resolution camera. The typical crack velocities evaluated from the experiments are shown in Fig. 4. The highest crack velocity of around 800 m/s (see Fig. 4) is detected for the Test Nr. 12 (see Table 1). However, it should be noted that the precision of the estimation of crack velocity is limited by the resolution of the camera. The measurement of the crack velocity was performed by the high resolution camera FASTCAM APX-RS. From the crack initiation till crack branching was possible to make 6 photos in the sequence of 19 ms. The critical crack width was assumed to be 0.1 mm. It was possible to measure it from the available camera resolution and the corresponding measured frame window (area of measurement = 70 × 30 mm). The measured average crack velocity was approximately 420 m/s.

The measured reaction-displacement curves are plotted in Fig. 5. The displacement is measured at the contact between concrete surface and loading frame. As expected, with increase of displacement (loading) rate the peak reaction increases.

Although, due to technical reasons, the experimentally tested and numerically investigated geometries and material properties of CTS are not identical, the comparison between presented test results and numerical prediction (Ožbolt et al., 2011) shows excellent agreement. The differences between concrete properties from the experiment and the properties employed in the analysis were: $E_{c\_exp}/E_{c\_num} = 36/30$ (in GPa), $f_{c\_exp}/f_{c\_num} = 53/40$ (in MPa) and $f_{t\_exp}/f_{t\_num} = 3.8/3.5$ (in MPa). For illustration Fig. 6 shows measured and numerically predicted failure modes (crack branching). The numerical prediction and here presented test results are principally the same. Both show that with increase of loading rate direction of crack propagation is changing. Once the crack velocity reaches critical value there is crack branching or even multiple crack branching. Moreover, the measured crack velocity is in about the same range. Therefore, it can be concluded that the 3D finite element code used in Ožbolt et al. (2011) is predictive since at time of publication the test results were not known and also, according to our knowledge, no similar test results for concrete were published so far.

Table 3
Summary of numerical results.

Test Nr.	Displacement rate, analysis (m/s)	Tensile strength (MPa)	Fracture energy (J/m^2)	Strain rate (1/s)	Crack opening rate (m/s)
0	Quasi-static	3.45 (3.80[a])	45.20(65.00[a])	–	–
2	0.035	4.52	38.0	3.20	0.03
5	1.400	4.63	46.3	45.30	1.38
8	3.300	4.68	50.8	56.80	4.48
12	4.300	4.64	48.9	77.20	5.55

[a] : Constitutive law – quasi-static uni-axial tension.

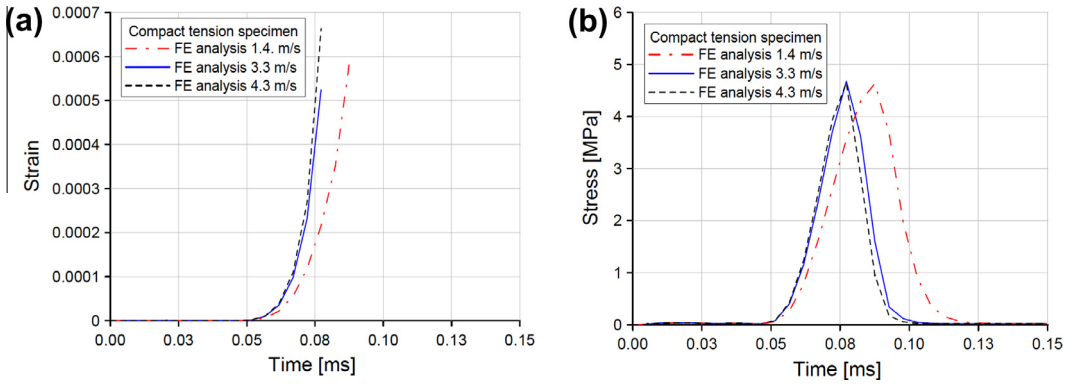

Fig. 11. Maximal principal strain and stress in the finite element where the crack is initiated.

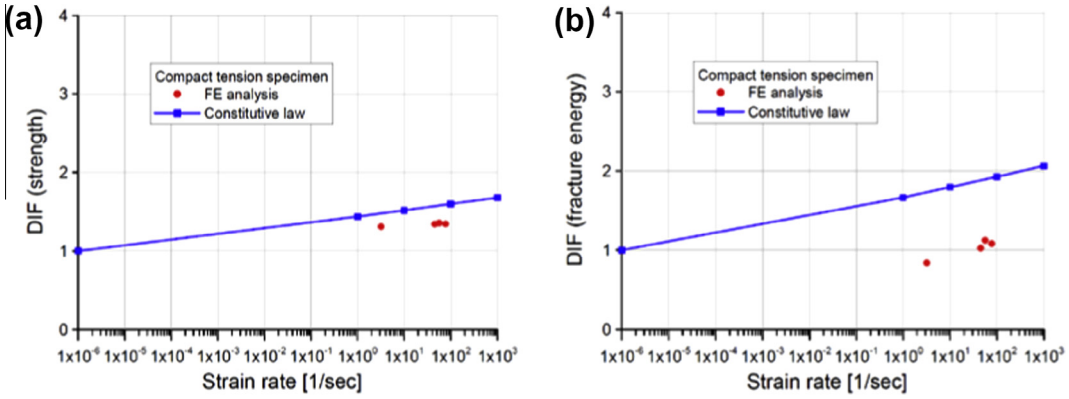

Fig. 12. DIF for tensile strength (a) and fracture energy (b) of concrete: measured in the finite element and resulting from the rate dependent constitutive law (microplane model).

3. Numerical analysis of tested CTS and comparison

In order to better interpret the results of the experimental tests, especially with respect to the crack velocity and strain rate, the above discussed tests are also simulated numerically. The numerical model exactly replicated the experimental setup. In the simulations the same 3D FE code that was used in Ožbolt et al. (2011) is employed. The code is explicit and based on the rate sensitive microplane model for concrete. The material properties, geometry, boundary conditions and loading are the same as in the experiment. In the FE discretization (see Fig. 7) four node solid finite elements are used. For steel loading and reaction frames linear elastic behavior is assumed. The contact between notch surface and steel plates is assumed to be perfect. The same as in the experiments, there is no contact between concrete side surfaces and loading frame. The displacement rates in the analysis are chosen such that corresponds to the experimental loading rates measured at the contact between loading plate and concrete.

3.1. Comparison between numerical and test results

The overview of numerical and experimental results for eight different loading rates is shown in Table 2. For the corresponding loading rates the numerically predicted maximum reaction forces and crack patterns are very similar. In Fig. 8 are compared crack patterns for quasi-static loading and for loading rates in the range between 35 and 4300 mm/s. As already discussed before, for quasi-static and relative low loading rates the crack is nearly horizontal (perpendicular to the loading direction), however, with increase of loading rate the crack becomes more inclined. The first crack branching in both cases is obtained for loading rate of 3.30 m/s. In Fig. 9 are shown predicted and experimentally obtained crack pattern with corresponding crack velocities (loading rate 4.30 m/s). For used properties of concrete maximum crack speed is around 800 m/s. As discuss in detail by Ožbolt et al. (2011), after crack velocity reaches critical speed (around 800 m/s) there is crack branching. Fig. 10 shows time evaluation of reaction for three different loading rates. It can be seen that there is very good agree-

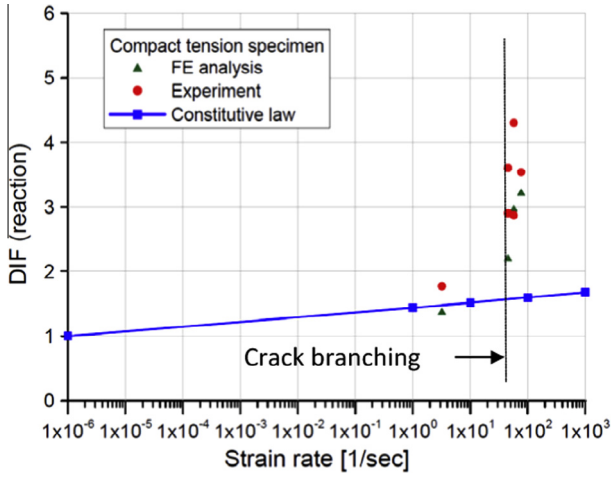

Fig. 13. DIF for reaction, predicted experimentally and numerically and compared with DIF for tensile strength of concrete from the rate dependent constitutive law (microplane model).

ment between numerical prediction and experiment. For quasi-static loading maximum reaction reaches approximately 1.60 kN and for loading rate of 4.30 m/s it is equal to approximately 5.90 kN, i.e. DIF (Dynamic Increase Factor) is equal to 3.69. The comparison between experimental and numerical results shows that the analysis is able to correctly replicate the test results.

In the tests on concrete specimen loaded by high strain rates is difficult to measure strain rate, the rate of crack opening, rate dependent tensile strength and fracture energy. Since it is confirmed that numerical analysis is able to simulate tests realistically, the above mentioned quantities are here obtained from the evaluation of numerical results.

In Table 3 are summarized results of numerical analysis. The properties listed in Table 3 are evaluated at the notch tip, in the finite element where the crack initiates. In Fig. 11 are plotted max. principal strains and corresponding max. principal stresses as a function of time for different loading rates. The rate dependent tensile strength and fracture energy shown in Table 3 are calculated from these curves. Note that the tensile strength and fracture energy evaluated for quasi-static loading at notch tip is slightly lower than obtained directly from the uni-axial tensile constitutive law. This can probably be attributed to the 3D effect at the notch tip which leads to three-dimensional tensile stress state.

The strain rate $d\varepsilon/dt$ is evaluated as a tangent on the principal strain history curve (Fig. 11a) at time at which tensile strength is reached (Fig. 11b). The rate of the crack opening dw/dt is calculated from the strain rate estimated after localization of crack, $dw/dt = (d\varepsilon/dt)\ h$, where h is the width of the crack band (equivalent element size) in the sense of the crack band approach (Bažant and Oh, 1983). From Table 3 can be seen that the crack opening approximately follows loading (displacement) rate, however, the strain rate increases much slower.

Fig. 12 shows DIF for measured tensile strength and fracture energy as a function of loading rate. As can be seen, the strength follows approximately the rate dependent constitutive law (Ožbolt et al., 2001, 2006). In contrast to this it is interesting to observe that DIF on fracture energy does not follow the rate dependent fracture energy from the constitutive law, i.e. it is almost independent of the strain rate. The reason for this could be the fact that, due to inertia forces at the crack tip, the part of the energy is consumed by damage that takes place before the crack is localized. Similar observation was made recently by the numerical evaluation of results obtained from simulation of Modified Split Hopkinson Bar experiment (Ožbolt et al., 2013).

In Fig. 13 is plotted DIF on reaction forces measured in the analysis and experiment as a function of strain rate. Up to the strain rate of approximately 50/s there is linear increase in DIF on resistance (reaction), which nicely follow the rate dependent constitutive law for tensile strength. Obviously, in this strain rate range reaction is controlled by the rate dependent constitutive law. However, for higher strain rates ($d\varepsilon/dt > 50$/s) there is progressive increase of reaction. Since the experimental and numerical results nicely agree, it can be concluded that the reason for the progressive increase cannot be the tensile strength and fracture energy, which show no progressive increase (see Fig. 12). As discussed in detail by Ožbolt et al. (2011) this progressive increase is controlled by structural inertia. Moreover, it is interesting to observe that the progressive increase of resistance coincides with the crack branching, which is experimentally and numerically observed for $d\varepsilon/dt > 50$/s. Consequently, it can be concluded that both phenomena are controlled by inertia.

4. Summary and conclusions

In the present article the influence of the loading rate on the concrete Compact Tension Specimen is experimentally and numerically studied. The tests are carried out in order to verify the results of numerical prediction performed recently by Ožbolt et al. (2011). Based on the evaluation of experimental and numerical results, the following can be concluded. (1) The evaluation of the test results confirms the results of numerical prediction. It is shown that relatively simple modeling approach based on continuum mechanics, rate dependent microplane model and standard finite elements is capable to realistically predict complex phenomena related to dynamic fracture of concrete. (2) Experiments and analysis show that the loading rate significantly influences the resistance and failure mode of the CTS. For strain rates, lower than approximately 50/s, the resistance is controlled by rate dependent constitutive law. However, for strain rates larger than 50/s influence of structural inertia dominate. (3) The progressive increase of resistance (reaction forces) for $d\varepsilon/dt > 50$/s is a consequence of inertia and is not related to the rate dependent strength of concrete, which is approximately linear in semi-log scale and is controlled by the constitutive law. (4) The evaluation on numerical results shows that fracture energy does not follow fracture energy dependency from the constitutive law, which is linear in semi-log scale. Instead, it is approximately independent of the strain rate. The reason is attributed to the 3D effect at the notch tip and related inertia forces that caused 3D tensile stress state. (5) For strain rates $d\varepsilon/dt < 50$/s the failure mode is due to mode-I fracture, however, for $d\varepsilon/dt > 50$/s mixed failure mode is observed. (6) The evaluation of test and numerical results show that for $d\varepsilon/dt > 50$/s there is crack branching. The phenomenon is related with progressive increase of resistance (reaction) and is also controlled by structural inertia. (7) The experiments and analysis confirm that crack velocity depends on the current crack pattern. For the here investigated concrete the highest measured crack velocity reaches approximately 800 m/s and is measured at the onset of crack branching. After crack branches the crack velocity drops down.

References

Banthia, N.P., Mindess, S., Bentur, A., 1987. Impact behaviour of concrete beams. Materials and Structures/Matériaux et Constructions 20, 293–302.
Bažant, Z.P., Oh, B.H., 1983. Crack band theory for fracture of concrete. RILEM 93 (16), 155–177.
Bischoff, P., Perry, S., 1991. Compressive behaviour of concrete at high strain rates. Materials and Structures/Matériaux et Constructions 24, 425–450.
fib, (2012). New Model Code, Chapter 5, Code-type models for concrete behavior (Final Draft).
Curbach, M., Eibl, J., 1990. Crack velocity in concrete. Engineering Fracture Mechanics 35 (1–3), 321–326.

Dilger, W.H., Koch, R., Kowalczyk, R., 1978. Ductility of Plain and Confined Concrete under Different Strain Rates. American Concrete Institute, Detroit, Michigan, USA, Special publication.

Freund, L.B., 1972a. Crack propagation in an elastic solid subjected to general loading-I. Constant rate of extension. Journal of the Mechanics and Physics of Solids 20, 129–140.

Freund, L.B., 1972b. Crack propagation in an elastic solid subjected to general loading-II. Non-uniform rate of extension. Journal of the Mechanics and Physics of Solids 20, 141–152.

Larcher, M., 2009. Development of discrete cracks in concrete loaded by shock waves. International Journal for Impact Engineering 36, 700–710.

Ožbolt, J., Li, Y., Kožar, I., 2001. Microplane model for concrete with relaxed kinematic constraint. International Journal of Solids and Structures 38, 2683–2711.

Ožbolt, J., Reinhardt, H.W., 2005. Rate dependent fracture of notched plain concrete beams. In: Pijaudier-Cabot, Gerard, Acker (Eds.), Proceedings of the 7th international conference CONCREEP-7, 57–62.

Ožbolt, J., Rah, K.K., Mestrović, D., 2006. Influence of loading rate on concrete cone failure. International Journal of Fracture 139, 239–252.

Ožbolt, J., Sharma, A., Reinhardt, H.W., 2011. Dynamic fracture of concrete – compact tension specimen. International Journal of Solids and Structures 48, 1534–1543.

Ožbolt, J., Sharma, A., 2012. Numerical simulation of dynamic fracture of concrete through uni-axial tension and L-specimen. Engineering Fracture Mechanics 85, 88–102.

Ožbolt, J., Sharma, A., Sola, E., 2013. Tensile behaviour of concrete under high loading rates, Submitted for publication in International Journal of Impact Engineering.

Rabczuk, T., Belytschko, T., 2004. Cracking particles: a simplified mesh free method for arbitrary evolving cracks. International Journal for Numerical Methods in Engineering 61, 2316–2343.

Rabczuk, T., Eibl, J., Stempniewski, L., 2004. Numerical analysis of high speed concrete fragmentation using a mesh free Lagrangian method. Engineering Fracture Mechanics 71, 547–556.

Pedersen, R.R., 2009. Computational Modelling of Dynamic Failure of Cementitious Materials, Dissertation, TU Delft, the Netherlands.

Reinhardt, H.W., 1982. Concrete under impact loading, Tensile strength and bond. Heron, 27, No.3.

Travaš, V., Ožbolt, J., Kožar, I., 2009. Failure of plain concrete beam at impact load: 3D finite element analysis. International Journal of Fracture 160, 31–41.

Weerheijm, J., 1992. Concrete under Impact Tensile Loading and Lateral Compression, Dissertation, TU Delft, the Netherlands.